Journal of Materials Chemistry C

PAPER

View Article Online
View Journal | View Issue

Cite this: J. Mater. Chem. C, 2014, 2, 884

Rubrene analogues with the aggregation-induced emission enhancement behaviour†

Xiaotao Zhang,[a] Jakob K. Sørensen,[b] Xiaolong Fu,[a] Yonggang Zhen,*[a] Guangyao Zhao,[a] Lang Jiang,[a] Huanli Dong,*[a] Jie Liu,[a] Zhigang Shuai,[c] Hua Geng,[a] Thomas Bjørnholm[b] and Wenping Hu*[a]

Received 11th September 2013
Accepted 13th November 2013

DOI: 10.1039/c3tc31794c

www.rsc.org/MaterialsC

In the light of the principle of aggregation-induced emission enhancement (AIEE), the rubrene analogue with orange light-emitting properties is designed and synthesized by substituting the phenyl side groups of rubrene with thienyl groups. To the best of our knowledge, this is the first report on the synthesis of rubrene with AIEE behaviour, thus paving the way for the development of light-emitting rubrene derivatives.

1. Introduction

Rubrene, a benchmark organic semiconductor with extremely high charge carrier mobility and excellent electroluminescent properties, has found important applications in organic field effect transistors (OFETs) as an active layer and in organic light-emitting diodes (OLEDs) as a doping layer.[1–3] Although rubrene is highly fluorescent in solutions, it becomes weakly luminescent along with the increase of concentration or aggregation in the solid state due to the formation of fluorescent quenching species such as exciplexes or excimers, which prevents the use of rubrene in OLEDs as the active neat layer. Therefore, the design and synthesis of rubrene-based materials which possess significant luminescence in the solid state is of great interest and importance.

Using the principle of aggregation-induced emission (AIE) and aggregation-induced emission enhancement (AIEE) proposed by the groups of Tang and Park is a very effective strategy to construct light-emitting materials.[4–6] Very recently, we synthesized 11,11,12,12-tetracyano-9,10-anthraquinodimethane derivatives with AIEE behaviour by the restriction of the rotation of the substituted phenyl rings in the solid state.[7] Herein, we introduced thienyl lateral groups to the tetracene backbone to achieve the orange light-emitting rubrene analogues by maintaining a distorted molecular conformation, confining the rotations and preventing the π···π stacking in the solid state. Furthermore, in contrast to rubrene,[8–13] the thienyl substituted rubrenes showed very high photo-oxidation stability upon exposure to light and oxygen under ambient conditions. To the best of our knowledge, this is the first report on the synthesis of rubrene analogues with AIEE properties, thus paving the way for the development of orange light-emitting rubrene derivatives.

2. Experimental section

2.1 Synthesis

Compound 2: 1,1-diphenyl-3-(thiophen-2-yl)prop-2-yn-1-ol. *n*-BuLi (1.6 M in THF, 6.9 mL, 1.1 equiv.) was added to a solution of 2-ethynylthiophene (10 mmol, 1.0 equiv.) in dry THF at −78 °C under the atmosphere of argon. After the resulting solution was stirred for 40 min at −78 °C, a solution of benzophenone (10 mmol, 1 equiv.) in dry THF was added slowly. After 15 min, the resulting solution was slowly warmed up to room temperature and stirred for another 10 h. Finally, the resulting mixture was quenched by saturated aqueous NH_4Cl (10 mL) and extracted with CH_2Cl_2 (3 × 30 mL). The combined organic layers were washed with brine (20 mL), dried with $MgSO_4$, concentrated under reduced pressure, and purified by flash column chromatography on silica gel (eluent: *n*-hexane–CH_2Cl_2 = 1 : 2) to give brown solids of the title compound (**2**) (7.5 mmol, yield: 75%). ^{1}H NMR (400 MHz, $CDCl_3$) δ (ppm): 7.69 (d, 4H), 7.38 (t, 4H), 7.32 (d, 4H), 7.01 (s, 1H), 2.97 (s, 1H). ^{13}C NMR (100 MHz, $CDCl_3$) δ (ppm): 145.23, 133.12, 128.87, 128.64, 128.34, 128.13, 127.87, 127.74, 127.72, 127.55, 126.59, 122.76, 95.90, 81.10, 75.54. HR-MS (EI) for $C_{19}H_{14}OS$: calculated: 290.3789; found: 290.3784.

Compound 3: 2,2′-(6,12-diphenyltetracene-5,11-diyl)dithiophene. Propargyl alcohol **2** (2.9 g, 10 mmol, 10 equiv.) was dissolved in dry toluene (30 mL) with moderate heating, then the solution was cooled and stirred at 0 °C under a nitrogen atmosphere. Triethylamine (NEt_3) (2.0 mL, 14 mmol, 14 equiv.) and benzenesulfonyl chloride ($PhSO_2Cl$) (1.5 mL, 11.7 mmol, 11.7 equiv.) were added dropwise to the solution successively to

[a]Beijing National Laboratory for Molecular Sciences, Key Laboratory of Organic Solids, Institute of Chemistry, Chinese Academy of Sciences, Beijing 100190, China. E-mail: zhenyg@iccas.ac.cn; dhl522@iccas.ac.cn; huwp@iccas.ac.cn

[b]Nano-Science Center and Department of Chemistry, University of Copenhagen, Universit etsparken 5, 2100, Copenhagen, Denmark

[c]Department of Chemistry, Tsinghua University, Beijing 100084, P. R. China

† Electronic supplementary information (ESI) available. CCDC 917691 and 917692. For ESI and crystallographic data in CIF or other electronic format see DOI: 10.1039/c3tc31794c

keep the temperature of the reaction below 10 °C. After the addition, the solution was stirred at 0 °C for 15 min, then warmed up to room temperature for 15 min and then heated to 110 °C for 4 h. Finally, the reaction was cooled, diluted with ethyl acetate (100 mL) and washed with 2.0 M HCl. The organic layers were collected, dried over $MgSO_4$, concentrated under reduced pressure, and purified by flash column chromatography on silica gel (eluent: *n*-hexane) to give red solids of the title compound (**3**) (544 mg, 1 mmol, yield: 20%). ^{1}H NMR (400 MHz, $CDCl_3$) δ (ppm): 7.52 (s, 3H), 7.35 (s, 3H), 7.11 (s, 12H), 6.85 (s, 2H), 6.67 (s, 2H), 6.39 (s, 2H). ^{13}C NMR (100 MHz, $CDCl_3$) δ (ppm): 141.99, 138.78, 132.63, 131.95, 131.09, 130.83, 128.70, 127.80, 127.22, 126.73, 126.20, 125.70. HR-MS (EI) for $C_{38}H_{24}S_2$: calculated: 544.7272; found: 544.7260. Elemental analysis calculated for $C_{38}H_{24}S_2$ (%): C, 83.79; H, 4.44. found: C, 83.48; H, 4.46.

Compound 5: 5,6,11,12-tetra(thiophen-2-yl)-5,12-dihydrotetracene-5,12-diol. Thiophen-2-yllithium (1.0 M in THF, 4.6 mL, 2.3 equiv.) was added to a solution of 6,11-di(thiophen-2-yl) tetracene-5,12-dione (**4**) (2 mmol, 1.0 equiv.) in dry THF at −78 °C under the atmosphere of argon. The resulting solution was stirred for 0.5 h at −78 °C, then slowly warmed up to room temperature and stirred for another 10 h. Finally, the reaction mixture was quenched by saturated aqueous NH_4Cl (10 mL) and extracted with CH_2Cl_2 (3 × 30 mL). The combined organic layers were washed with brine (20 mL), dried over $MgSO_4$, concentrated under reduced pressure, and purified by flash column chromatography on silica gel (eluent: *n*-hexane–CH_2Cl_2 = 2 : 1) to give pale yellow solids of the title compound (**5**) (0.7 mmol, yield: 35%). ^{1}H NMR (400 MHz, $CDCl_3$) δ (ppm): 7.62 (s, 2H), 7.53 (d, 3H), 7.36–7.30 (m, 3H), 7.21–7.00 (m, 7H), 6.97 (s, 1H), 6.71 (s, 2H), 6.48 (d, 2H), 6.04 (d, 1H), 4.49 (s, 1H). ^{13}C NMR (100 MHz, $CDCl_3$) δ (ppm): 140.46, 138.76–138.30, 135.97, 134.46, 132.55, 129.27, 128.93, 127.10, 126.79, 126.51, 126.08, 125.86, 125.53. HR-MS (EI) for $C_{34}H_{20}O_2S_4$: calculated: 590.7973; found: 590.7965.

Compound 6: 5,6,11,12-tetra(thiophen-2-yl)tetracene. A suspension of compound **5** (590 mg, 1 mmol, 1 equiv.), ZnI_2 (1.01 g, 3.4 mmol) and $NaBH_3CN$ (0.69 g, 11 mmol, 11 equiv.) in 1,2-dichloroethane (8 mL) was refluxed under an argon atmosphere in the dark for 24 h. After the reaction mixture was cooled to room temperature, dichloromethane (30 mL) was added and the solids were filtered off. The clear filtrate was washed with diluted HCl (3 M, 3 × 20 mL) dried over Na_2SO_4, then concentrated in a vacuum. The residue was purified by column chromatography on silica gel (eluent: *n*-hexane) to give red solids of compound **6** (84 mg, yield: 15%). ^{1}H NMR (400 MHz, $CDCl_3$) δ (ppm): 7.61 (s, 4H), 7.28 (d, 4H), 7.26–7.22 (m, 4H), 6.88 (d, 4H), 6.68 (s, 4H). ^{13}C NMR (100 MHz, $CDCl_3$) δ (ppm): 131.27, 128.50, 125.31, 124.91. HR-MS (EI) for $C_{34}H_{20}S_4$: calculated: 556.7826; found: 556.7812. Elemental analysis calculated for $C_{34}H_{20}S_4$ (%): C, 73.34; H, 3.62. Found: C, 73.19; H, 3.68.

2.2 Measurement and characterization

^{1}H-NMR and ^{13}C-NMR spectra were recorded on a Bruker DMX-400 spectrometer. Chemical shifts were reported in ppm relative to the singlet of $CDCl_3$ at 7.26 ppm and 77 ppm for ^{1}H-NMR and ^{13}C-NMR respectively. UV-vis spectra were obtained on a JΛSCO V-570 UV-vis spectrometer. Photoluminescence (PL) spectra were recorded on a Perkin-Elmer LS 55 spectrofluorometer. Absolute quantum yield measurement (LabSphere®, FluoroMax-4, HORIBA Jobin Yvon, PLQY software package) was used for powder samples. In this experimental setup, it is possible to measure the Photoluminescence Quantum Yields (PLQY) *via* using the integrating sphere in combination with a commercial fluorimeter. Emission spectra including the scattering region of excitation light were recorded for both blank and test samples, and these spectra were corrected with instrumental factors to calculate the quantum yield. Cyclic voltammograms were recorded on a CHI660C electrochemistry station using tetrabutylammonium hexafluorophosphate (Bu_4NPF_6) as the supporting electrolyte (0.001 M in dry CH_2Cl_2). The working, counter and reference electrodes were glassy carbon, Pt wire and Ag/AgCl, respectively. Thermogravimetric analysis (TGA) was performed on a PERKIN ELMER TGA7 apparatus with the scanning rate of 10 °C min^{-1}. X-Ray diffraction measurements were obtained in reflection mode at 40 kV and 200 mAwith Cu Kα radiation using a 2 kW Rigaku D/max-2500 X-ray diffractometer.

3. Results and discussion

The synthetic routes for the compounds are shown in Scheme 1. A novel two-step route different from previous methods[14–17] is designed for the synthesis of compound **3**. Two molecules of compound **2** involved a condensation reaction in the presence of benzene-sulfonyl chloride and triethylamine to give the target molecule **3** in the total yield of 15%. Compound **5** was synthesized with the yield of 35% after addition of thiophene to the carbonyl carbon of compound **4**.[17] Finally compound **6** was synthesized by removal of the hydroxyl group and aromatization in 1,2-dichloroethane using zinc iodide and sodium cyanoborohydride as reducing agents.

3.1 Photophysical properties

UV-vis absorption spectra and cyclic voltammograms of the compounds are shown in Fig. 1. The compounds exhibit similar

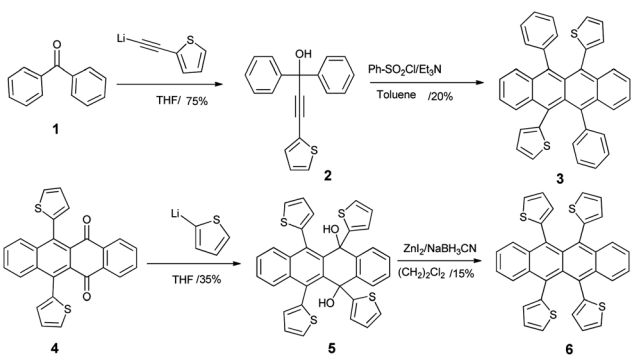

Scheme 1 Synthetic route to compounds **3** and **6**.

absorption characteristics to that of rubrene (Fig. 1). The absorption peaks at around 301 nm attributed to the tetracene backbone exhibit no obvious shift although there is an absorption shoulder for compound **3**. Compared with rubrene, compounds **3** and **6** showed a slight red-shift in the region of 450–550 nm. The maximum absorption edges for rubrene, compound **3** and compound **6** are 551 nm, 564 nm and 574 nm, respectively, indicating that their energy gaps are 2.25, 2.20, and 2.16 eV, respectively. The variation of their energy gaps is less than 0.1 eV.

Surprisingly, by adding water into the tetrahydrofuran (THF) solution, the luminescence intensity of compound **3** was enhanced by more than 40 times, while that of rubrene decreased sharply (Fig. S9 in ESI†). As shown in Fig. 2, only very weak PL intensity was observed in the THF–water solution of **3** when the fraction of water was no higher than 40 vol%. However, the PL intensity was swiftly promoted with a water fraction of 50 vol%. However, the PL intensity decreased when the water fraction was above 90 vol% (Fig. 2C), this might be caused by different aggregate formation.[7] Since water is a non-solvent of **3**, the molecules must have aggregated in the mixture, demonstrating the obvious AIEE behaviour. The observation suggested that with the addition of water into THF the molecules of **3** may slowly assemble in an ordered fashion which was more emissive, like crystalline clusters. The absolute fluorescence quantum yield of the solid state is determined to be 7% by a calibrated integrating sphere.

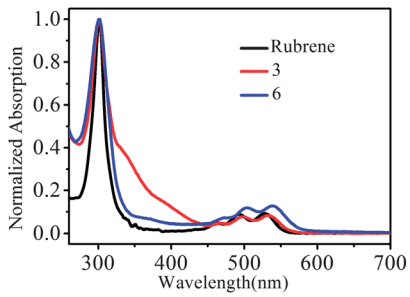

Fig. 1 UV-vis spectra of compounds **3**, **6** and rubrene.

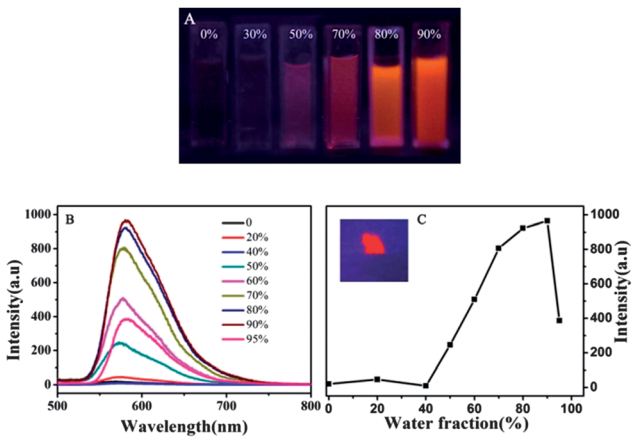

Fig. 2 (A) PL pictures of **3** solutions with different water fractions under UV (365 nm) light. (B) PL spectra of **3** in different water–THF (v/v) mixtures. (C) The dependence of the PL intensity on the composition of water (inset: luminescent photo of the solid powder under 365 nm). The concentration was kept at 40 μM, excitation wavelength: 470 nm.

3.2 Electrochemical properties

The redox properties of rubrene, compounds **3** and **6** are shown in Fig. 3, and their highest occupied molecular orbital (HOMO) levels are calculated to be −5.16, −5.19 and −5.24 eV by the onsets of oxidation peaks, while their lowest unoccupied molecular orbital (LUMO) levels are estimated to be −2.90, −2.98 and −3.08 eV by the onsets of reduction peaks, respectively. The energy gaps for rubrene, compounds **3** and **6** calculated from cyclic voltammograms are consistent well with the absorption spectra (Table 1). In comparison with rubrene, compounds **3** and **6** showed lower HOMO levels, which rendered the compounds higher ionization potential and more difficult to proceed the oxidation, leading to the higher stability from a theoretical point of view.[18]

3.3 Anti-photooxidation properties

Rubrene, compounds **3** and **6** exhibit different colors in the same solvent.[19] For example, in CH_2Cl_2, rubrene exhibits an orange, while compound **3** displays reddish orange and compound **6** appears as a peach color. Therefore, a vivid way to judge the stability of the compounds is to expose their solutions to air for some time to observe the change in their colors. The results are shown in Fig. 4. It was obvious that the solution of rubrene became colorless in 2 hours, while the compounds **3** and **6** exhibit no obvious color change even after exposure to air

Table 1 HOMO–LUMO levels and energy gaps of compounds **3**, **6** and rubrene

	$E_{ox,onset}$ [eV]	$E_{red,onset}$ [eV]	HOMO[a] [eV]	LUMO[a] [eV]	E_g[b] [eV]
R	0.36	−1.90	−5.16	−2.90	2.26
3	0.39	−1.82	−5.19	−2.98	2.21
6	0.44	−1.72	−5.24	−3.08	2.16

[a] HOMO levels were estimated by the onsets of oxidation peaks *vs.* Fc/Fc^+ from CV, HOMO = −4.8 − $E_{ox,onset}$; LUMO levels were estimated by the onsets of reduction peaks *vs.* Fc/Fc^+ from CV, LUMO = −4.8 − $E_{red,onset}$. [b] The energy gaps were calculated from cyclic voltammograms.

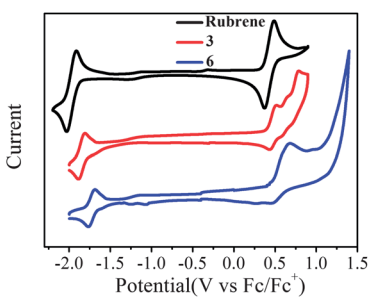

Fig. 3 Cyclic voltammogram curves of compounds **3**, **6** and rubrene.

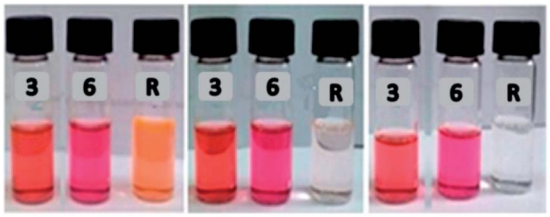

Fig. 4 The color changes of rubrene (R), compounds 3 and 6 in CH_2Cl_2 (5 mM) solutions after exposure to air over 2 and 50 hours.

over 50 hours. These results vividly suggested the excellent stability of compounds 3 and 6 as shown in Fig. 4.

The UV-vis absorption spectra of these solutions under white light illumination in air were examined as shown in Fig. 5. The absorption spectra of rubrene exhibited obvious change in the region of 250–350 nm and 450–550 nm in 2 hours, indicating the fast degradation of rubrene in solution in air. After 50 hours, no absorption peaks are observed for rubrene except the absorption shoulder at around 301 nm. However, for compounds 3 and 6, no obvious changes in their absorption spectra are observed as shown in Fig. 5B and 5C, indicating the high stability of the solution of the rubrene analogies. The results agreed well with the color change of their solutions as shown in Fig. 5, indicating the strong stability against photo-oxidization in solution.

The thin film stability of rubrene, compounds 3 and 6 is evaluated using the UV-vis absorption spectra under white light illumination in air as shown in Fig. 6. A similar degradation trend was observed in the thin film of rubrene (Fig. 6A). After 23 hours, no absorption peaks are observed for the rubrene thin film except the small absorption shoulder at around 301 nm. In contrast to rubrene, compounds 3 and 6 showed no obvious changes in their absorption spectra in Fig. 6B and C. The results agreed well with that of their solutions as shown in Fig. 4 and 5, verifying the strong stability of compounds 3 and 6 against photo-oxidization both in solution and thin films, which is especially important for the potential application of the compounds in organic electronic devices.

3.4 Thermal stability

Besides the high environmental stability, compounds 3 and 6 also exhibited excellent thermal stability with decomposition temperatures as high as 301 °C and 324 °C respectively as shown in Fig. 7. The observation indicates their potential use in high temperature cases.

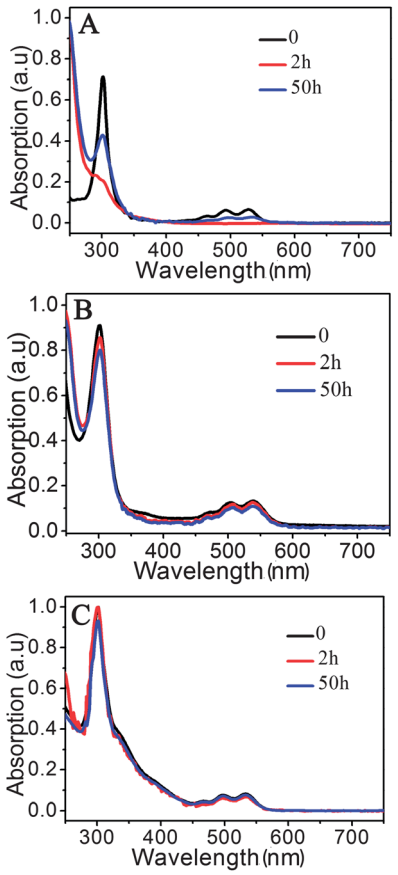

Fig. 5 UV-vis spectra of solution of rubrene, compounds 3 and 6 in air (A: rubrene, B: compound 3, C: compound 6, in CH_2Cl_2, 0.1 M).

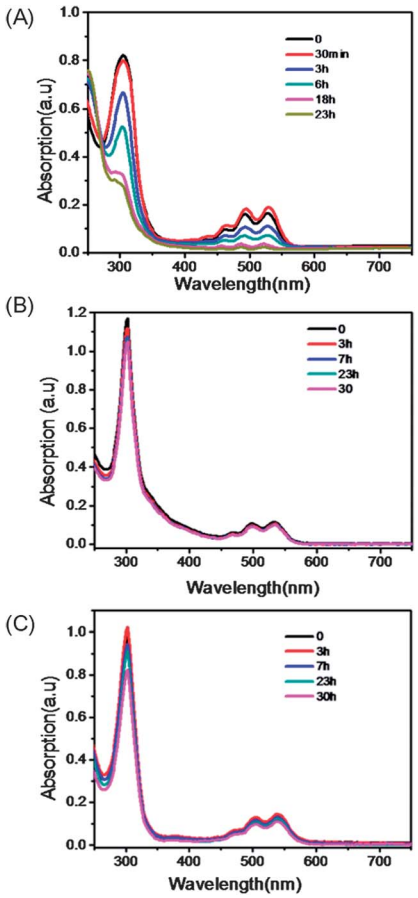

Fig. 6 UV-vis spectra of thin films of rubrene, compounds 3 and 6 in air (A: rubrene, B: compound 3, C: compound 6, 100 nm thin films on quart).

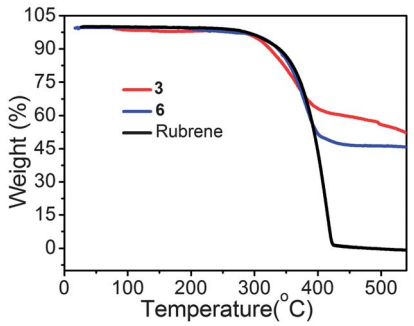

Fig. 7 TGA curves of compounds **3**, **6** and rubrene, measured with a heating rate of 10 °C min^{-1} in nitrogen.

3.5 Computation by DFT theory

In order to clarify the mechanism for the improvement of the stability of the novel rubrene analogues,[20] density functional theory (DFT) calculations are performed with Gaussian03 at the B3LYP/6-31 G (d) level. As shown in Fig. 8, the largest coefficients in the HOMO of rubrene (**R**) are mainly located on the tetracene core, while those of compounds **3** and **6** show similar electronic structure in the tetracene core with moderate coefficients on thienyl rings, which is presumably one important contribution to the photostability.

3.6 X-ray crystal structures

Our previous studies[21,22] suggested that the introduction of thiophene rings in organic semiconductors could lead to a variety of intra- and intermolecular interactions such as sulfur–sulfur interactions and hydrogen bond interactions, which in turn results in the improved stability of the compounds due to the prevention of molecular shape change by these abundant intra- and inter-molecular interactions. In order to investigate the inter- and intra-molecular interactions of these compounds, single-crystal X-ray structure analyses are performed. Suitable single crystals of compounds **3** and **6** are grown by using mixture solvents (CH_2Cl_2–toluene = 1 : 5 v/v) through slow evaporation at room temperature. XRD patterns demonstrated that these compounds crystallized in a space group of a simple monoclinic system. Table 2 shows the crystal data and structural refinement of compounds **3** and **6**. Indeed, as shown in Fig. 9, both compounds **3** and **6** exhibit abundant intra- and inter-molecular interactions including C–H···π, S···C, and C–H···S interactions, while rubrene exhibits much more intermolecular H···H short contacts. The difference of the short contacts between rubrene and compounds **3** and **6** is probably another reason for the improved stability of compounds **3** and **6**.

Moreover, the abundant intra- and inter-molecular interactions have obvious effect on the spatial configuration. The

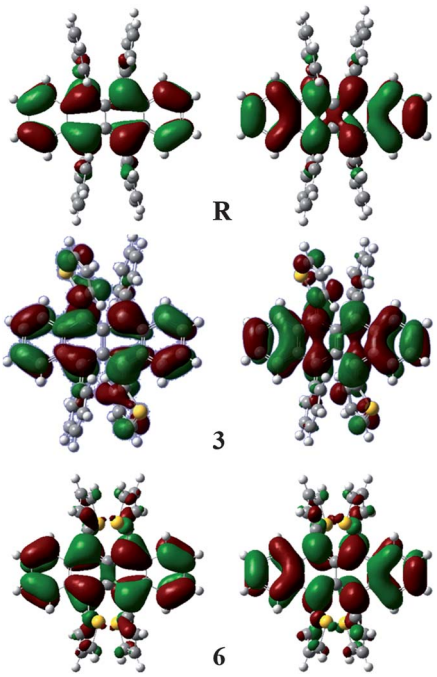

Fig. 8 HOMO (left) and LUMO (right) orbitals of rubrene (**R**), compounds **3** and **6** calculated by DFT theory.

Table 2 Single crystal diffraction data and structural refinement for compounds **3** (CCDC 917691) and **6** (CCDC 917692)

Parameters	**3**	**6**
Empirical formula	$C_{38}H_{24}S_2$	$C_{34}H_{20}S_4$
Formula weight	544.69	556.74
Temperature	173(2) K	173(2) K
Wavelength	0.71073	0.71073
Crystal system	Monoclinic	Monoclinic
Space group	*P*2(1)/*c*	*P*2(1)
Unit cell dimensions	a = 10.173(2) Å, α = 90.00 b = 8.9148(18) Å, β = 95.17(3) c = 14.751(13) Å, γ = 90.00	a = 11.401(2) Å, α = 90.00 b = 8.9944(18) Å, β = 113.59(3) c = 13.989(3) Å, γ = 90.00
Z	2	2
Density (calculated)	1.358 g cm^{-3}	1.406 mg m^{-3}
Absorption coefficient	0.228	0.385
F(000)	568	576
Crystal size (mm)	0.21 × 0.18 × 0.16	0.42 × 0.29 × 0.17
Theta range for data collection	3.04° to 27.48°	1.59° to 27.48°
Index ranges	$-11 \le h \le 13$ $-11 \le k \le 10$ $-19 \le l \le 19$	$-14 \le h \le 14$ $-9 \le k \le 11$ $-18 \le l \le 13$
Reflections collected	10 474	10 807
Independent reflections	3037	5637
R_{int}	0.0500	0.0518
Completeness to theta	99.3%	99.8%
Absorption correction	Multi-scan	Multi-scan
Max. and min. transmission	1.00 and 0.6809	1.00 and 0.3970
Data/restraints/parameters	3037/38/195	5637/367/380
Goodness-of-fit on F^2	1.173	1.045
Final R indices [I > 2sigma(I)]	R_1 = 0.0649 wR_2 = 0.1292	R_1 = 0.0430 wR_2 = 0.1025
R indices (all data)	R_1 = 0.0712 wR_2 = 0.1326	R_1 = 0.0449 wR_2 = 0.1041
Largest diff. peak and hole	0.347 and −0.516 e $Å^{-3}$	0.359 and −0.235 e $Å^{-3}$

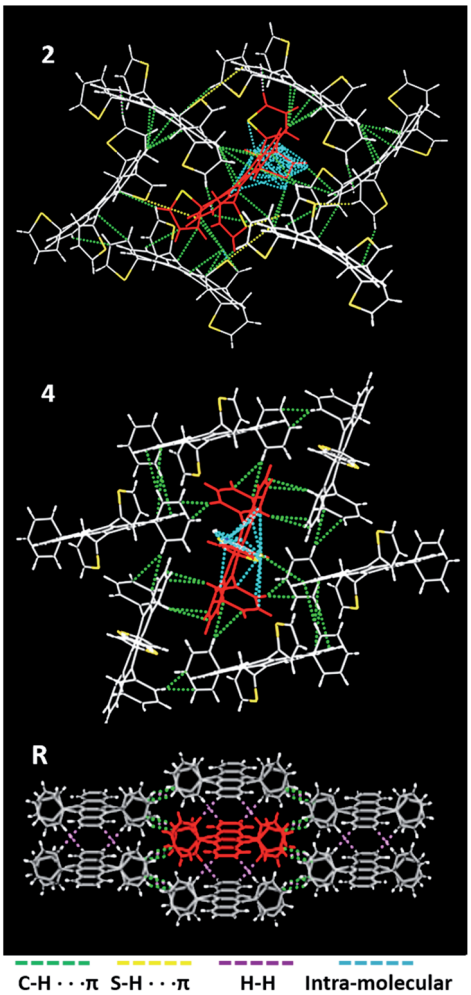

Fig. 9 Inter- and intra-molecular short contacts of compounds **3**, **6** and rubrene (intra-molecular short contacts include C–H and S–H short contacts).

backbone of rubrene is planar and four phenyl groups are twisted strongly out of the planar backbone like wings. However, for compound **3**, two side phenyl groups are replaced by two thienyl groups at 6- and 12-carbon positions with dihedral angles of 88.5° or 89.2° between thienyl or phenyl groups and the tetracene backbone respectively, and the backbone slightly twisted. These characteristics are favourable to lower the potential energy of the molecules and make negligible influence on the conjugation of the molecules,[23,24] finally leading to the improvement of the stability of the compounds. For compound **6**, four side phenyl groups of rubrene are all replaced by thienyl groups, which further enhances the intra- and inter-molecular interactions and lowers the potential energy of the molecules, hence improving the stability of the compound.[25,26]

4. Conclusions

In summary, two rubrene anti-photooxidation analogues, compounds **3** and **6**, are designed and synthesized efficiently by substituting the phenyl groups of rubrene with thienyl groups. The lower activity of the tetracene core by shifting partial electron clouds to the thienyl side groups accounts for the extremely high stability. Very interestingly, compound **3** exhibits AIEE properties by maintaining a distorted molecular conformation, confining the rotations and preventing the π···π stacking in the solid state. This is the first report on the AIEE properties of a rubrene derivative, paving the way for the exploration of rubrene-based AIEE-active materials. Further structure modifications and device applications are underway.

Acknowledgements

The authors acknowledge the financial support from National Natural Science Foundation of China (20721061, 51033006, 51222306, 51003107, 61201105, 91027043, 91222203, 91233205), the China-Denmark Co-project, TRR61 (NSFC-DFG Transregio Project), the Ministry of Science and Technology of China (2011CB808400, 2011CB932300, 2013CB933403, 2013CB933500) and the Chinese Academy of Sciences.

Notes and references

1 (*a*) C. Wang, H. Dong, W. Hu, Y. Liu and D. Zhu, *Chem. Rev.*, 2012, **112**, 2208–2267; (*b*) H. Dong, C. Wang and W. Hu, *Chem. Commun.*, 2010, **46**, 5211–5222.

2 (*a*) V. C. Sundar, J. Zaumseil, V. Podzorov, E. Menard, R. L. Willett, T. Someya, M. E. Gershenson and J. A. Rogers, *Science*, 2004, **303**, 1644–1666; (*b*) J. Takeya, M. Yamagishi, Y. Tominari, R. Hirahara, Y. Nakazawa, T. Nishikawa, T. Kawase, T. Shimoda and S. Ogawa, *Appl. Phys. Lett.*, 2007, **90**, 102120.

3 (*a*) J. W. Lee, K. Kim, D. H. Park, M. Y. Cho, Y. B. Lee, J. S. Jung, D.-C. Kim, J. Kim and J. Joo, *Adv. Funct. Mater.*, 2009, **19**, 704–710; (*b*) M. M. Richter, *Chem. Rev.*, 2004, **104**, 3003–3036; (*c*) A. S. Paraskar, A. R. Reddy, A. Patra, Y. H. Wijsboom, O. Gidron, L. J. W. Shimon, G. Leitusand and M. Bendikov, *Chem.–Eur. J.*, 2008, **14**, 10639–10647.

4 J. D. Luo, Z. L. Xie, J. W. Y. Lam, L. Cheng, H. Y. Chen, C. F. Qiu, H. S. Kwok, X. W. Zhan, Y. Q. Liu, D. B. Zhu and B. Z. Tang, *Chem. Commun.*, 2001, 1740–1741.

5 B. K. An, S. K. Kwon, S. D. Jung and S. Y. Park, *J. Am. Chem. Soc.*, 2002, **124**, 14410–14415.

6 Q. Zeng, Z. Li, Y. Q. Dong, C. A. Di, A. J. Qin, Y. N. Hong, L. Ji, Z. C. Zhu, C. K. W. Jim, G. Yu, Q. Q. Li, Z. A. Li, Y. Q. Liu, J. G. Qinand and B. Z. Tang, *Chem. Commun.*, 2007, 70–72.

7 J. Liu, Q. Meng, X. Zhang, X. Lu, P. He, L. Jiang, H. Dong and W. Hu, *Chem. Commun.*, 2013, **49**, 1199–1201.

8 (*a*) L. Jiang, H. Dong and W. Hu, *J. Mater. Chem.*, 2010, **20**, 4994–5007; (*b*) R. W. I. de Boer, M. E. Gershenson, A. F. Morpurgo and V. Podzorov, *Phys. Status Solidi A*, 2004, **201**, 1302–1331; (*c*) S. Seo, B.-N. Park and P. G. Evans, *Appl. Phys. Lett.*, 2006, **88**, 232114; (*d*) D. A. S. Filho, E.-G. Kim and J.-L. Bredas, *Adv. Mater.*, 2005, **17**, 1072–1076; (*e*) A. L. Briseno, S. Mannsfeld, M. Ling, S. Liu, R. J. Tseng, C. Reese, M. Roberts, Y. Yang, F. Wudl and Z. Bao, *Nature*, 2006, **444**, 913–917; (*f*)

Y. Zhang, H. Dong, Q. Tang, W. Chen, S. Ferdous, F. Liu, S. C. B. Mannsfeld, W. Hu and A. L. Briseno, *J. Am. Chem. Soc.*, 2010, **132**, 11580–11584; (*g*) A. L. Briseno, S. Mannsfeld, X. Liu, Y. Xiong, S. A. Jenekhe, Z. Bao and Y. Xia, *Nano Lett.*, 2007, **7**, 668–675.

9 (*a*) R. M. Hochstrasser and M. Ritchie, *Trans. Faraday Soc.*, 1956, **52**, 1363–1373; (*b*) R. M. Hochstrasser, *Can. J. Chem.*, 1959, **37**, 1123–1125; (*c*) E. L. Frankevich, M. M. Tribel and I. A. Sokolik, *Phys. Status Solidi B*, 1976, **77**, 265–276; (*d*) Y. Harada, T. Takahashi, S. Fujisawa and T. Kajiwara, *Chem. Phys. Lett.*, 1979, **62**, 283–286.

10 (*a*) K. Ohno, H. Mutoh and Y. Harada, *Surf. Sci.*, 1982, **115**, L128–L132; (*b*) M. Kytka, A. Gerlach, F. Schreiber and J. Kovac, *Appl. Phys. Lett.*, 2007, **90**, 131911; (*c*) O. Mitrofanov, D. V. Lang, C. Kloc, J. M. Wikberg, T. Siegrist, W.-Y. So, M. A. Sergent and A. P. Ramirez, *Phys. Rev. Lett.*, 2006, **97**, 166601.

11 (*a*) C. H. Hsu, J. Deng, C. R. Staddon and P. H. Beton, *Appl. Phys. Lett.*, 2007, **91**, 193505; (*b*) Y. Chen and I. Shih, *Appl. Phys. Lett.*, 2009, **94**, 083304; (*c*) S.-W. Park, S. H. Jeong, J.-M. Choi, J. M. Hwang, J. H. Kim and S. Im, *Appl. Phys. Lett.*, 2007, **91**, 033506.

12 A. A. Virkar, S. Mannsfeld, Z. Bao and N. Stingelin, *Adv. Mater.*, 2010, **22**, 3857–3875.

13 M. Yamada, I. Ikemoto and H. Kuroda, *Bull. Chem. Soc. Jpn.*, 1988, **61**, 1057–1062.

14 X. Zhang, W. T. Teo and P. W. H. Chan, *Org. Lett.*, 2009, **11**, 4990–4993.

15 H. W. Gibson, S. H. Lee, P. T. Engen, P. Lecavalier, J. Sze, Y. Shen and M. Bheda, *J. Org. Chem.*, 1993, **58**, 3748–3756.

16 (*a*) Y. Zhu, S. Wen, G. Yin, D. Hong, P. Lu and Y. Wang, *Org. Lett.*, 2011, **13**, 3553; (*b*) P. Essenfeld, US. Pat. No. 4855520, 1989; (*c*) P. Essenfeld, Eur. Pat. No. 0302195, 1989.

17 X. Zhang, Q. Meng, Y. He, C. Wang, H. Dong and W. Hu, *Sci. China: Chem.*, 2011, **54**, 631–635.

18 J. Poater, R. Visser, M. Sola and F. M. Bickelhaupt, *J. Org. Chem.*, 2007, **72**, 1134.

19 H. Wonneberger, C.-Q. Ma, M. A. Gatys, C. Li, P. Baeuerle and K. Mullen, *J. Phys. Chem. B*, 2010, **114**, 14343–14347.

20 J. Nortonand and K. N. Houk, *J. Am. Chem. Soc.*, 2005, **127**, 4162–4163.

21 K. Xiao, Y. Liu, T. Qi, W. Zhang, F. Wang, J. Gao, W. Qiu, Y. Ma, G. Cui, S. Chen, X. Zhan, G. Yu, J. Qin, W. Hu and D. Zhu, *J. Am. Chem. Soc.*, 2005, **127**, 13281–13286.

22 J. Gao, R. Li, L. Li, Q. Meng, H. Jiang, H. Li and W. Hu, *Adv. Mater.*, 2007, **19**, 3008–3011.

23 M. Kaupp, M. Renz, M. Parthey, M. Stolte, F. Wurthner and C. Lambert, *Phys. Chem. Chem. Phys.*, 2011, **13**, 16973–16986.

24 A. S. Paraskar, A. R. Reddy, A. Patra, Y. H. Wijsboom, O. Gidron, L. J. W. Shimon, G. Leitus and M. Bendikov, *Chem.–Eur. J.*, 2008, **14**, 10639–10647.

25 Y. Hou, X. Chi, X. Wan and Y. Chen, *J. Mol. Struct.*, 2008, **889**, 265–270.

26 M. M. Safont-Sempere, P. Osswald, M. Stolte, M. Grune, M. Renz, M. Kaupp, K. Radacki, H. Braunschweig and F. Wurthner, *J. Am. Chem. Soc.*, 2011, **133**, 9580–9891.

